Broadbanding of a Planar Antenna with Three Frequency Bands and Its Application

Hiroyasu Matsui and Toshio Wakabayashi

This paper describes a line element planar antenna with three frequency bands. To obtain broadband characteristics, a modified planar antenna that has semi-elliptical elements based on the characteristics of a line element planar antenna is proposed and analyzed by the finite difference time domain method. Return loss characteristics are discussed as functions of the eccentricity values of semi-ellipse at each element. The broadbanding of the modified planar antenna is implemented based on the results. The planar antenna with three systems (an 800 MHz band cellular phone, a third-generation cellular phone, and a 2.4 GHz band wireless LAN system) is considered as an application example.

Keywords: Planar antenna, three-frequency bands, broadbanding, FDTD.

I. Introduction

The development of multi-functionality in the field of electronic devices has been remarkable. The cellular phone additionally functions as a global positioning system (GPS) receiver and a TV receiver. Notebook computers often include a TV receiver and several wireless boards. In such cases, planar antennas with multi-frequency bands are desired. Also, small conformal planar antennas are desirable because of their flexible exterior design and ease of carrying. Many types of planar antennas have been studied [1], [2].

There are two types of antenna which cover several frequency bands. One is the broadband antenna, the other is the multiband antenna. The broadband antenna can include several desired frequency bands; however, it is difficult to adapt polarization characteristics for each wireless communication system. The multiband antenna has resonant frequencies at several desired frequency bands. For adaptability to multifunctional electronic devices, the line element planar antenna with three frequency bands printed on the dielectric substrate has been studied [3]. Generally, with this type of antenna, the frequency bandwidth is narrow; however, the structure is simple and it is easy to design and adjust. Therefore, it is necessary to widen the bandwidth at each resonant frequency of a multiband antenna to correspond to the bandwidth for each wireless communication system.

The planar antenna with broadband characteristics or multi-frequency bands has been studied for wireless communication systems. One method of obtaining broadband characteristics is to change the element shape [4]-[6]. A multiband antenna that combines the Bluetooth system and the wireless LAN system with several mobile phone systems has been developed [7], [8], and the design of multiband microstrip antennas has been

Manuscript received May 25, 2007; revised Oct. 10, 2007.

Hiroyasu Matsui (phone: + 81 463 58 1211, email: 7akc1008@keyaki.cc.u-tokai.ac.jp) is with the Graduate School of Engineering, Tokai University, Kanagawa, Japan.

Toshio Wakabayashi (email: wakaba@dt.u-tokai.ac.jp) is with the School of Information Science and Engineering, Tokai University, Kanagawa, Japan.

studied [9], and techniques for effective broadband and multiband antennas have been proposed [2]. In order to improve the adaptability to multi-functionality, an antenna with features of both a broadband antenna and a multi-band antenna should be studied.

In this paper, we propose a modified planar antenna with three frequency bands for wireless communication systems and analyze it by the finite difference time domain (FDTD) method. The antenna is converted to broadband by changing the shape of the antenna elements while maintaining the independence of each resonant characteristic. And broadband characteristic is considered for the shapes of the antenna elements. The return loss is discussed using the eccentricity of the semi-ellipse at each element. Moreover, an antenna that combines an 800-MHz-band cellular phone, a third-generation cellular phone, and a 2.4-GHz-band wireless LAN (IEEE 802.11b) system is considered for future wireless communications as an application example. The characteristics of return loss and radiation patterns are described for both analytical and measured results.

II. Structure of a Planar Antenna with Three Frequency Bands

Figure 1 depicts the basic structure of the line element planar antenna with three frequency bands. This antenna has the ground plane and the antenna elements on the same side of the dielectric substrate. In this structure, a conductor is printed on the left-hand side of the dielectric substrate as a ground plane, and the antenna elements are printed on the right-hand side. The feeding point is placed between the ground plane and the antenna elements. The substrate is L_g+L_d in length, W_g in width, and h in thickness.

The antenna consists of three elements. Element A is L_1 in length and contacts the feeding point. Element C consists of two parts that are L_{31} and L_{32} in length. Here, L_{31} is part of element A, and L_{32} is connected vertically to element A.

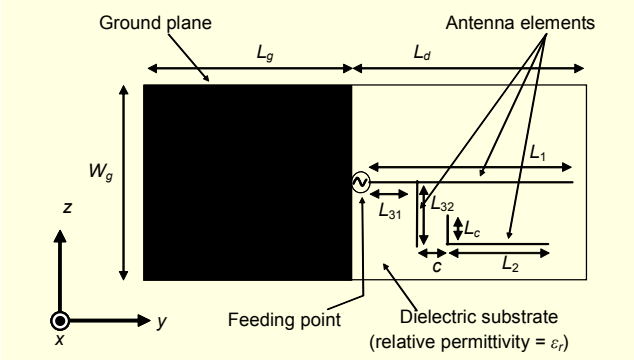

Fig. 1. Basic structure of planar antenna with three frequency bands.

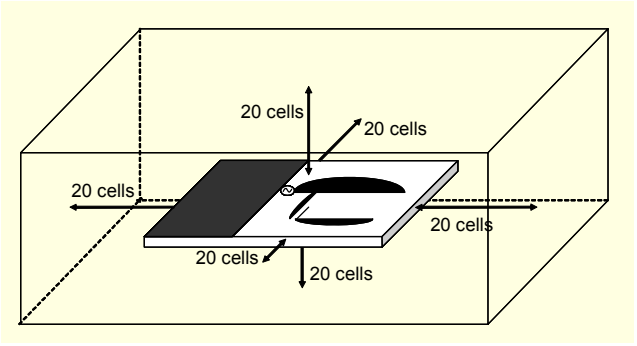

Fig. 2. Analytical region.

Element B has a structure that is bent to form the L letter, and it consists of two parts that are L_2 and L_c in length. Further, a part of length L_c is positioned at distance c from element C.

III. Analytical Method

The FDTD method was used to analyze the object antenna. The cell size is dx=dy=dz, and the input is a Gaussian pulse. The perfectly matched layer (PML) absorbing boundary condition is applied to boundaries, and it consists of eight layers. Twenty cells are taken as a distance between the antenna and the wall of the analytical region in each direction as shown in Fig. 2 [10]. Moreover, the time step satisfies the Courant stability condition:

$$dt \le \frac{1}{c_0\sqrt{\left(\frac{1}{dx}\right)^2+\left(\frac{1}{dy}\right)^2+\left(\frac{1}{dz}\right)^2}}, \qquad (1)$$

where c_0 is velocity of light.

For the FDTD analysis, the analytical tool in [11] and [12] was used, and the accuracy of FDTD analysis has been confirmed in these references. The cell size was 1 mm in the analysis, and the semi-elliptical elements, which are described later, were approximated with step form. This result is compared with results for the case of 0.5 mm cell size in section VI.

IV. Basic Characteristics of a Planar Antenna with Three Frequency Bands

Figure 3 plots the return loss of the three-frequency-band planar antenna presented in Fig. 1, which was analyzed by the FDTD method. The antenna has three resonant frequencies, which depend on the parameters of the antenna as follows [3].

(a) If only L_1 is changed, the first resonant frequency (f_1) and the third resonant frequency (f_3) shift, but the second resonant frequency (f_2) does not move.

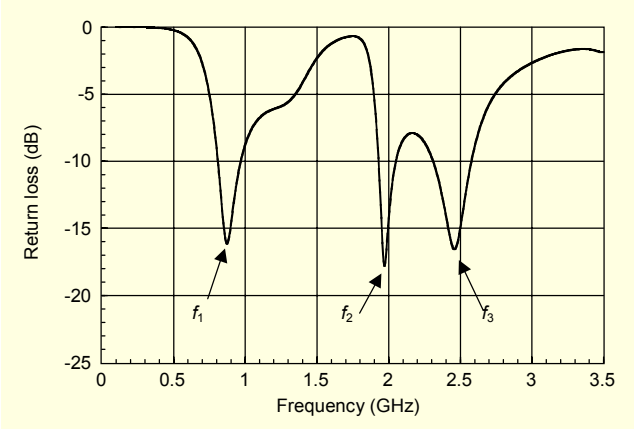

Fig. 3. Return loss of basic structure (L_g=85, L_d=79, W_g=60, L_1=63, L_2=45, L_{31}=12, L_{32}=13, L_c=2, c=1, h=1 mm, ε_r=4.2).

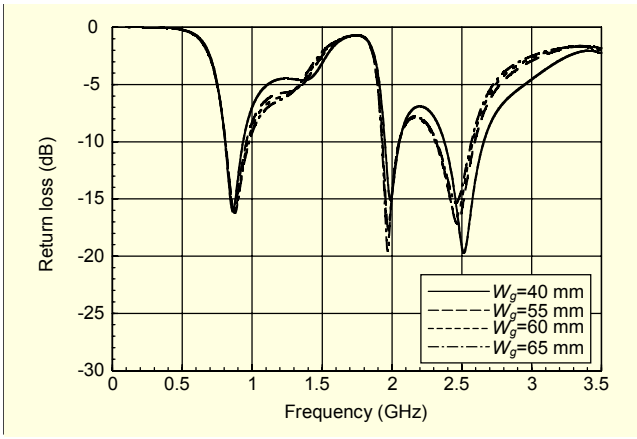

Fig. 4. Return loss with changing of W_g (L_g=85, L_d=79, L_1=63, L_2=45, L_{31}=12, L_{32}=13, L_c=2, c=1, h=1 mm, ε_r=4.2).

(b) If only L_2 is changed, f_2 changes, but f_1 and f_3 do not.
(c) If only L_{31} is changed, only f_2 shifts.
(d) If only L_{32} is changed, f_2 and f_3 shift without moving f_1.
(e) Only when L_c is changed, f_2 shifts; f_1 and f_3 do not move.
(f) If c is changed, only f_2 shifts.

From these descriptions, we can state the following:

(i) The first resonant frequency depends on L_1.
(ii) The second resonant frequency mainly depends on L_2, L_{32}, L_c, and c.
(iii) The third resonant frequency mainly depends on L_1 and L_{32}.

Figures 4 and 5 show changes of return loss for W_g and L_g, respectively. From Fig. 4, it is confirmed that even if the length of W_g changes, the return loss characteristics are almost the same, and the characteristic of three resonant frequencies is maintained. However, the antenna needs the length of W_g, which is more than twice of length of L_{32}, due to the limitation of the structure to obtain the effective three resonant

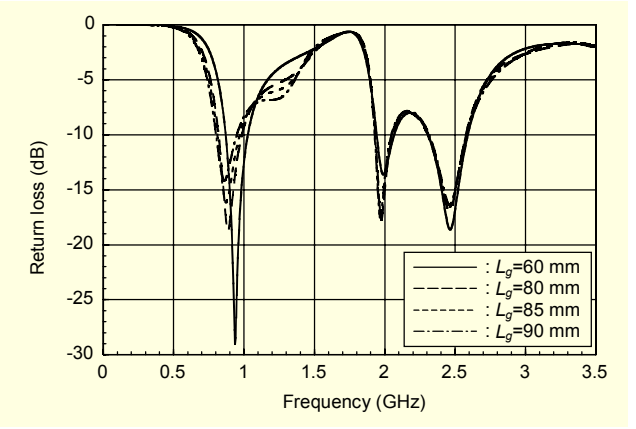

Fig. 5. Return loss with changing of L_g (L_d=79, W_g=60, L_1=63, L_2=45, L_{31}=12, L_{32}=13, L_c=2, c=1, h=1 mm, ε_r=4.2).

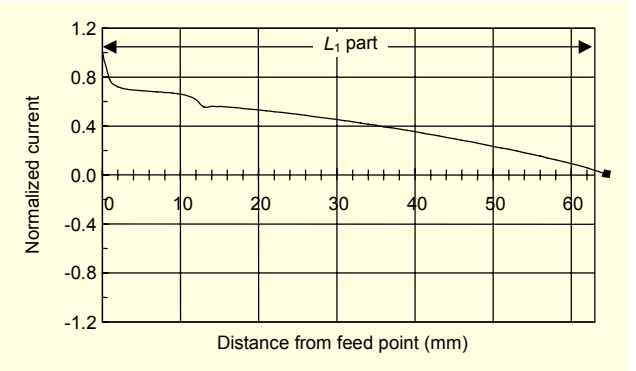

Fig. 6. Current distribution at the first resonant frequency on element A (L_1 part: L_g=85, L_d=79, W_g=60, L_1=63, L_2=45, L_{31}=12, L_{32}=13, L_c=2, c=1, h=1 mm, ε_r=4.2).

frequencies characteristic. Figure 5 indicates that the effective characteristic is obtained when the length of L_g is longer than the length of L_1. In this study, in order to investigate the basic characteristics in many frequency bands for the proposed planar antenna, the values of W_g=60 mm and L_g=85 mm were used.

V. Resonant Mechanism of a Planar Antenna with Three Frequency Bands

To consider the resonant mechanism of the planar antenna with three frequency bands, the current distribution on the antenna element (Fig. 1), on which each resonant frequency depends, is used [3]. A resonant mechanism is described by referring to the resonant characteristic of the planar dipole antenna printed on the dielectric substrate, which has the same dielectric constant as the planar antenna with a three-frequency-band antenna.

1. First Resonant Frequency

Figure 6 plots the current distribution for element A (L_1 part)

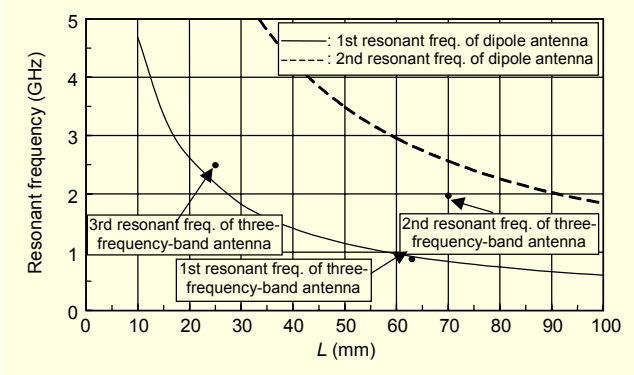

Fig. 7. Curves of resonant frequency of planar dipole antenna.

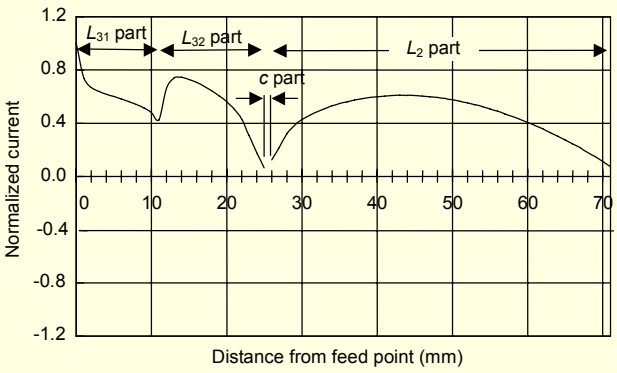

Fig. 8. Current distribution at the second resonant frequency on elements C and B (L_{31}, L_{32}, and L_2: L_g=85, L_d=79, W_g=60, L_1=63, L_2=45, L_{31}=12, L_{32}=13, L_c=2, c=1, h=1 mm, ε_r=4.2).

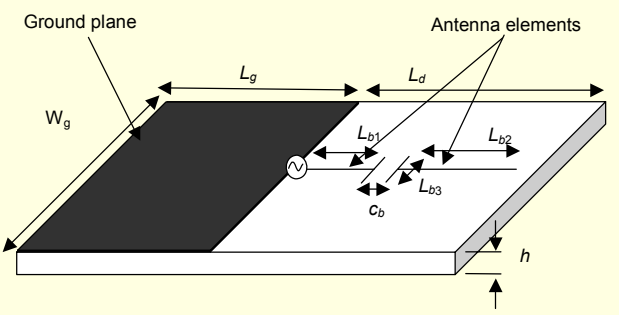

Fig. 9. Structure of a planar monopole antenna with a gap.

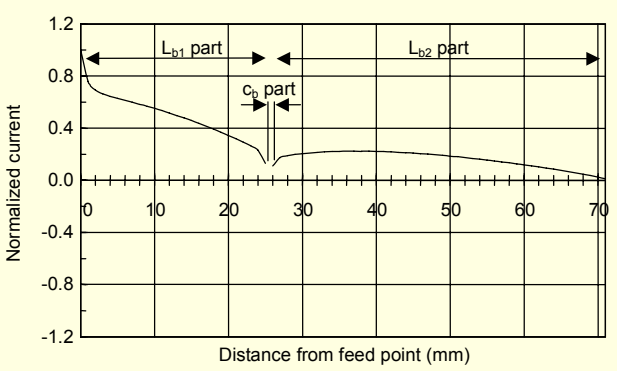

Fig. 10. Current distribution at resonant frequency of a planar monopole antenna with a gap (L_g=85, L_d=79, W_g=60, L_{b1}=25, L_{b2}=45, L_{b3}=2, c_b=1, h=1 mm, ε_r=4.2).

at the first resonant frequency, where the 0 mm point of the horizontal axis denotes the feeding point position. The current is normalized with the maximum current at the resonant frequency. In the normalized current value, the positive values indicate the current which goes to the tip of the element from the feeding point. The negative values indicate the current which goes to the feeding point from the tip of the element, and the phase is inverted for a positive value. The current at the first resonant frequency distributes without phase inversion on L_1, and the current is zero at the tip of element A.

The resonant frequency for element length $2L$ of one side of the planar dipole antenna printed on the dielectric substrate is presented in Fig. 7. The solid line denotes the first resonant frequency of the planar dipole antenna, and the dashed line denotes the second resonant frequency. The first resonant frequency of the planar antenna with three frequency bands for length L_1 is plotted as the first resonant frequency of the three-frequency-band antenna. This point is in agreement with the first resonant frequency curve of the planar dipole antenna. Results confirm that the wavelength at the first resonant frequency of the planar antenna with three frequency bands is $4L_1$.

2. Second Resonant Frequency

Figure 8 plots the current distribution on elements C and B (L_{31}, L_{32}, and L_2 parts) at the second resonant frequency, where L_{31}, L_{32}, and L_2 are considered a direct line. As in Fig. 6, the 0 mm point of the horizontal axis denotes the feeding point. The sign of the normalized current values means the direction of the current. The distribution curve is broken to denote the gap c section between L_{32} and L_2.

The second resonant frequency of the planar antenna with three frequency bands for L_{31}+L_{32}+L_2 length is plotted as the second resonant frequency of the three-frequency-band antenna in Fig. 7. This point is not in agreement with the resonant frequency curve of the planar dipole antenna. However, the current is distributed without phase inversion on these parts, and the current is 0 at the tip of element B.

We consider the planar monopole antenna with a gap (see Fig. 9) in order to analyze the mechanism of the second resonant frequency. Here, L_{b1} is equivalent to the length of L_{31}+L_{32} (see Fig. 1). Likewise, L_{b2}, L_{b3}, and c_b are equivalent to L_2, L_c, and c, respectively.

Figure 10 plots current distribution at the resonant frequency

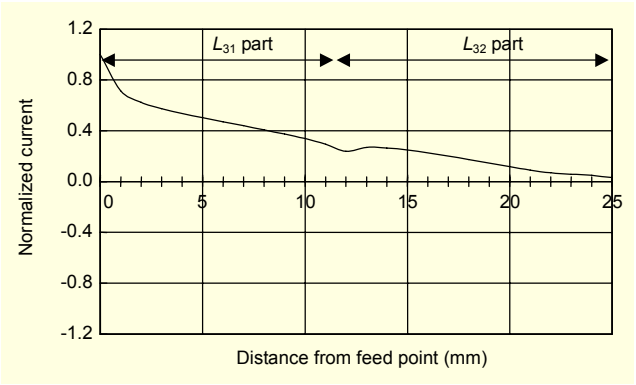

Fig. 11. Current distribution at the third resonant frequency on element C (L_{31} and L_{32} parts: L_g=85, L_d=79, W_g=60, L_1=63, L_2=45, L_{31}=12, L_{32}=13, L_c=2, c=1, h=1 mm, ε_r=4.2).

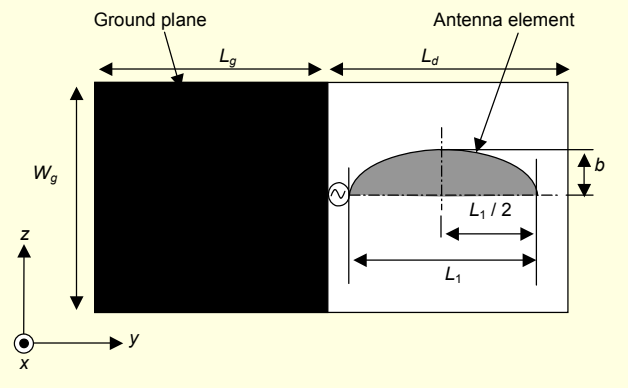

Fig. 12. Structure of planar monopole antenna with semi-elliptical element.

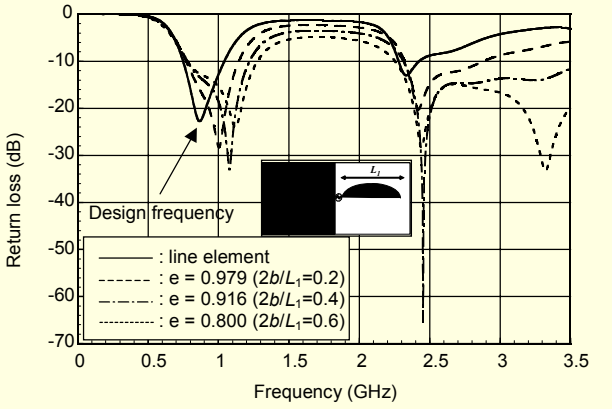

Fig. 13. Return loss of monopole antenna with semi-elliptical element (L_g=100, L_d=71, W_g=100, L_1=54, h=3 mm, ε_r=7.35).

of the planar monopole antenna with a gap. A comparison of Figs. 8 and 10 reveals that the styles of the current distributions are similar. Moreover, in the return loss of the planar antenna with three frequency bands, only the second resonant frequency shifts to the higher frequency side as distance c increases [3]. It is thought that this is due to the capacity of part c. Also, it is confirmed that the resonant frequency of this antenna shifts to the higher frequency side as c_b becomes larger.

These results reveal that the mechanism of the second resonant frequency of the planar antenna with three frequency bands is the same as that of the planar monopole antenna with a gap (see Fig 9).

3. Third Resonant Frequency

Figure 11 shows the current distribution on element C (L_{31} and L_{32}) at the third resonant frequency. The current at the third resonant frequency is distributed without phase inversion on L_{31} and L_{32}, and the current is zero at the tip of element C.

The third resonant frequency of a planar antenna with three frequency bands for L_{31}+L_{32} length is plotted as for the three-frequency-band antenna in Fig. 7. This point is almost in agreement with the first resonant frequency curve of the planar dipole antenna. The wavelength at the third resonant frequency of the planar antenna with three frequency bands is 4(L_{31}+L_{32}).

A line element planar antenna with three desired resonant frequencies is easily designed by considering this mechanism. Also, we can predict that to achieve a broad band at a desired resonant frequency, we should modify the element depending on the frequency.

VI. Broadbanding for Planar Antennas with Three Frequency Bands

1. Planar Monopole Antenna with Semi-Elliptical Element

Changing the shape of an antenna element from a line element to a circle or an ellipse is a known technique for making the antenna broadband [2]. This technique is employed to broaden each resonant frequency of a three-frequency-band planar antenna. However, it is difficult to change the shape of three line elements in a planar antenna with three frequency bands (see Fig. 1). Therefore, we consider the characteristics of a planar antenna with semi-elliptical elements.

It is possible to achieve a broadband planar antenna with three frequency bands by changing the shape of the antenna elements from lines to semi-ellipses. The part of an element that is L_1 in length is defined as element 1. Similarly, the part of an element that is length L_2 is defined as element 2, and that of length L_{32} is defined as element 3. Figure 12 illustrates an antenna that has an only one semi-elliptical element, element 1, with the following eccentricity e:

$$e = \sqrt{1 - \left(\frac{2b}{L_1}\right)^2}, \qquad (2)$$

where 2b is the minor axis of the antenna element.

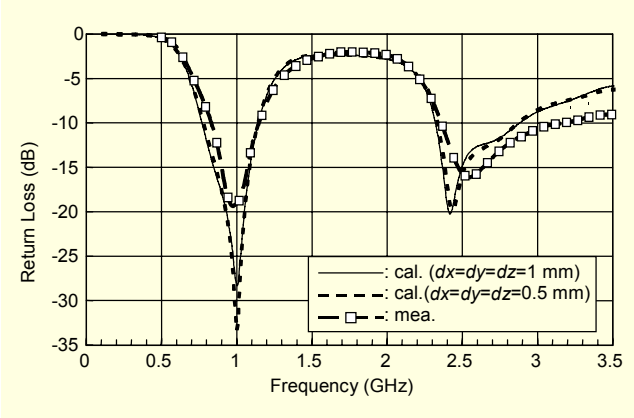

Fig. 14. Return loss of monopole antenna with semi-elliptical element in case of e=0.979 (L_g=100, L_d=71, W_g=100, L_1=54, h=3 mm, ε_r=7.35).

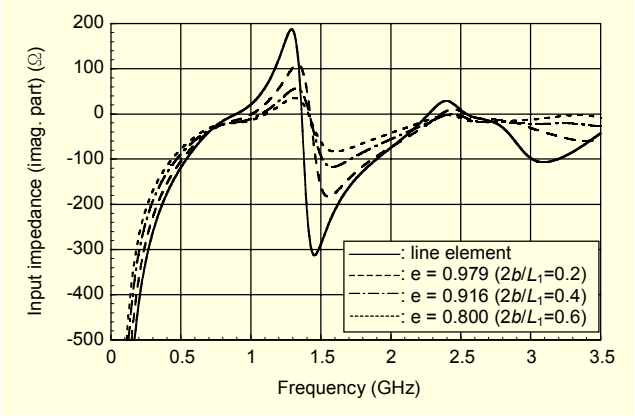

Fig. 16. Imaginary part of input impedance of planar monopole antenna with semi-elliptical element (L_g=100, L_d=71, W_g=100, L_1=54, h=3 mm, ε_r=7.35).

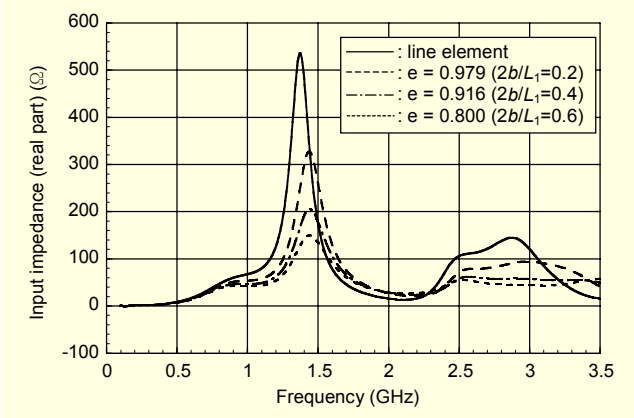

Fig. 15. Real part of input impedance of planar monopole antenna with semi-elliptical element (L_g=100, L_d=71, W_g=100, L_1=54, h=3 mm, ε_r=7.35).

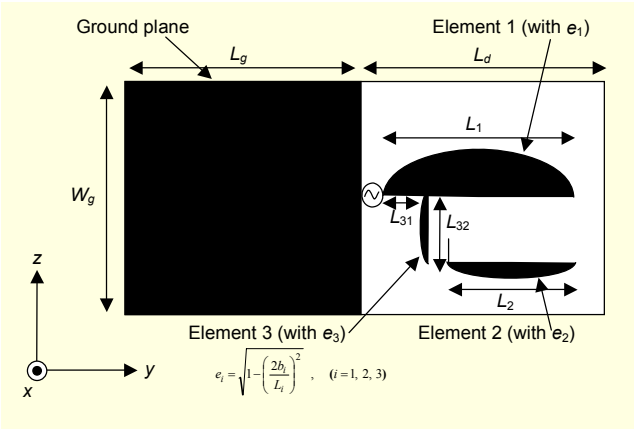

Fig. 17. Structure of modified planar antenna with three frequency bands.

Figure 13 plots the return loss for values of e. The planar monopole antenna is made broadband by changing the shape of element 1 from a line to a semi-ellipse. In this way, if the eccentricity becomes small (as b approaches $L_1/2$), a broadband antenna is obtained. However, the value of the return loss at the design frequency deteriorates in relation to the length of the line element.

Figure 14 compares the analytical results for the cases of dx=dy=dz=1 mm and dx=dy=dz=0.5 mm with the measured results. As the figure demonstrates, the return loss characteristics are almost the same in cases of 1 mm and 0.5 mm. Moreover, even if the semi-elliptical element is approximated with a step form, the analytical results and measured result are in agreement. Based on these results, the 1 mm cell size is also used for semi-elliptical elements.

We observed the input impedance in order to investigate the factors involved in making a broadband antenna. Figures 15 and 16 plot the real and imaginary input impedances of the planar antenna with a semi-elliptical element. As shown in Fig. 15, as e decreases, the characteristic curve of the real part of the input impedance approaches 50 ohms, and in Fig.16, the characteristic curve of the imaginary part approaches 0 ohms. Moreover, both characteristic curves increasingly flatten as e decreases. Broadband characteristics can be obtained by changing these input impedance characteristics.

The point at which the imaginary part crosses 0 shifts to the higher-frequency side as e decreases. This is a factor in the return loss deterioration at the design frequency.

These features are the same as those of the planar monopole antenna with an elliptical element. However, the input impedance for the elliptical element changes more with variations in e than that for the semi-elliptical element. Therefore, the elliptical element is more effective than the semi-elliptical element.

2. A Planar Antenna with Three Frequency Bands

As shown in Fig. 17, to realize our modified antenna, all

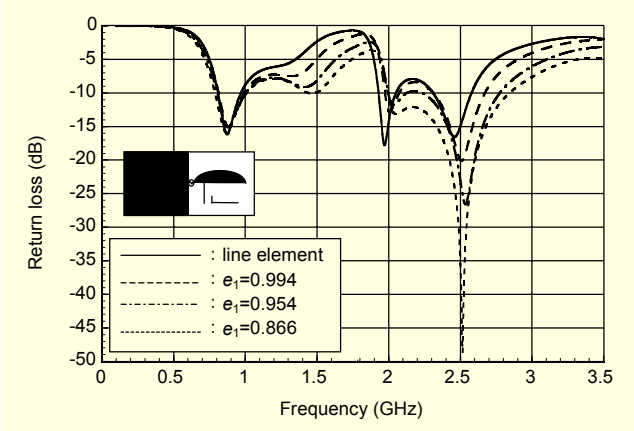

Fig. 18. Return loss when shape of element 1 is changed (L_g=85, L_d=79, W_g=60, L_1=63, L_2=45, L_{31}=12, L_{32}=13, L_c=2, c=1, h=1 mm, ε_r=4.2, e_2=e_3≈1).

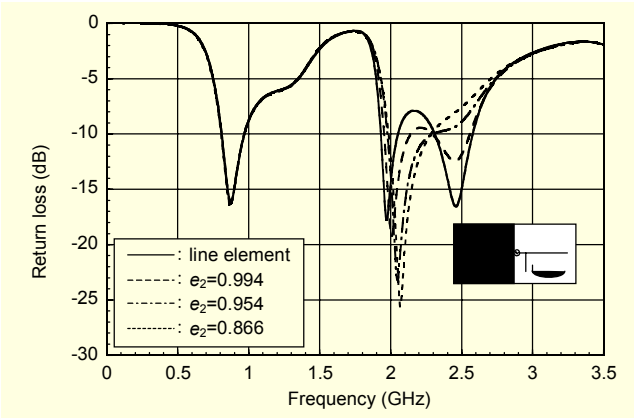

Fig. 19. Return loss when shape of element 2 is changed (L_g=85, L_d=79, W_g=60, L_1=63, L_2=45, L_{31}=12, L_{32}=13, L_c=2, c=1, h=1 mm, ε_r=4.2, e_1=e_2≈1).

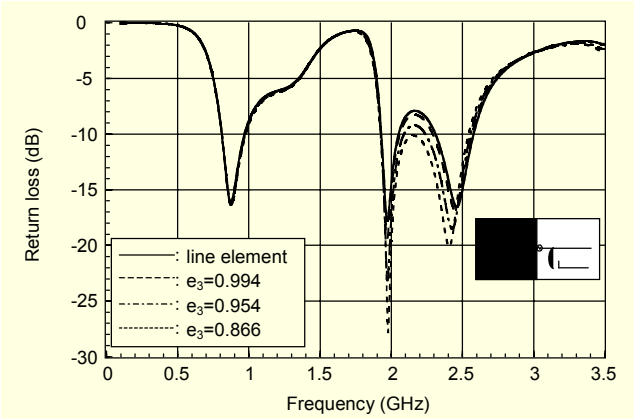

Fig. 20. Return loss when shape of element 3 is changed (L_g=85, L_d=79, W_g=60, L_1=63, L_2=45, L_{31}=12, L_{32}=13, L_c=2, c=1, h=1 mm, ε_r=4.2, e_1=e_2 ≈1).

elements are changed from lines to semi-ellipses. The eccentricities e_i (i=1, 2, 3) of element i are described as in (2),

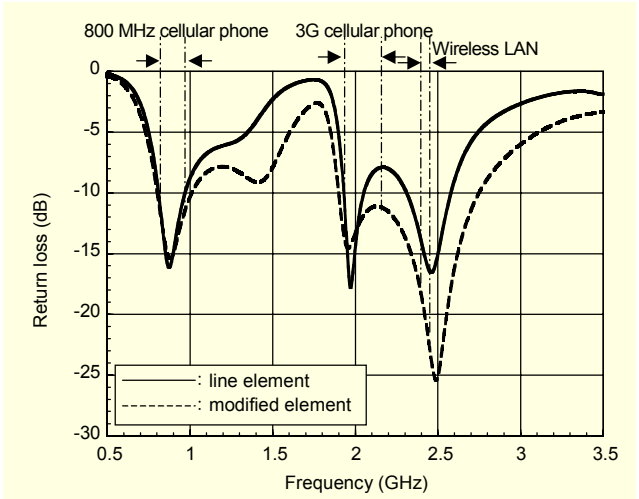

<Line element antenna>
L_g=85, L_d=79, W_g=60, L_1=63, L_2=45, L_{31}=12, L_{32}=13, L_c=2, c=1, h=1 mm, ε_r=4.2
<Modified element antenna>
L_g=85, L_d=79, W_g=60, L_1=63, L_2=45, L_{31}=12, L_{32}=13, L_c=4, c=1, h=1 mm, ε_r=4.2, e_1 = 0.953, e_2 = 0.994, e_3 = 0.866

Fig. 21. Return loss of a line element planar antenna and a modified element planar antenna.

where the major axis for element i (i=1, 2, 3) is given by L_i, and the minor axis is given by $2b_i$.

Figure 18 presents the broadband effect for the frequency bandwidth as parameter e_1. If only the shape of element 1 is changed, the bandwidths of the first and third resonant frequencies become broad, but the return loss at the second resonant frequency deteriorates. Figure 19 reveals the broadband effect for the frequency bandwidth as parameter e_2. If only the shape of element 2 is changed, the second resonant frequency becomes broad, but the return loss at the third resonant frequency deteriorates. Figure 20 presents the broadband effect for the frequency bandwidth when only e_3 is changed. When the shape of element 3 is changed, there is no change in bandwidth, but the return loss at the second and third resonant frequencies is improved.

These results indicate that the characteristics of the three resonant frequencies are not maintained by changing the shape of the antenna elements alone. Therefore, maintaining the three resonant frequencies and broad bandwidth requires the balancing of eccentricity e for each antenna element.

VII. Application to Three-Frequency-Band Antenna

As an application of the modified planar antenna with three frequency bands, the first resonant frequency is assigned to the 800 MHz band cellular phone (810 MHz to 957 MHz); the second resonant frequency is assigned to the third-generation cellular phone (1.92 GHz to 2.17 GHz); and the third resonant

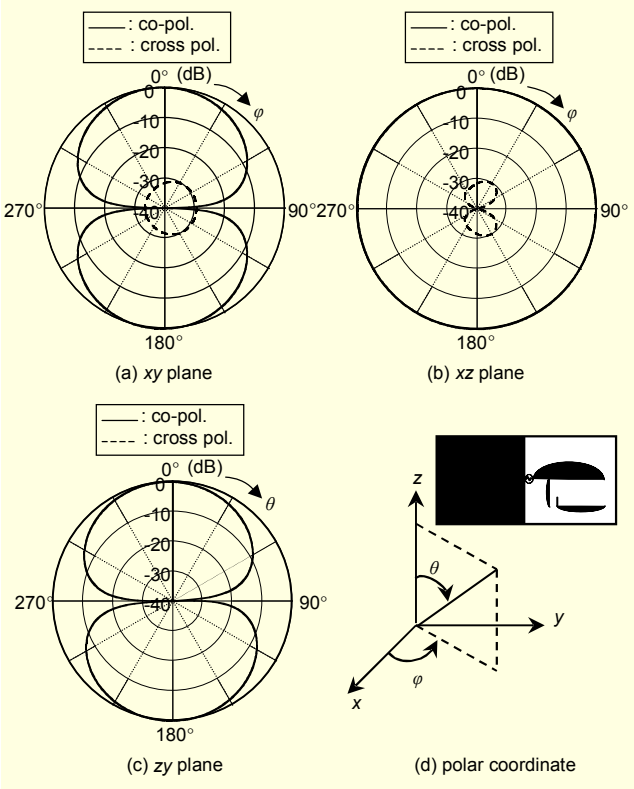

Fig. 22. Radiation patterns at the first resonant frequency and polar coordinate system.

frequency is assigned to the 2.4 GHz band wireless LAN (IEEE 802.11b; 2.40 GHz to 2.497 GHz). This is an example of a combined application.

Figure 21 plots the return loss of the modified planar antenna applied to three wireless communication systems. The frequency bandwidth of the modified planar antenna is broad at each resonant frequency, and the return loss is improved around the second and third resonant frequencies.

The radiation patterns are described next. The θ and φ axes of the polar coordinate system are defined as indicated in (d) of Fig. 22.

Figure 22 illustrates the radiation patterns of co-polarized and cross-polarized waves at the first resonant frequency. The co-polarized waves are electric field components E_φ in the *xy* plane and *xz* plane and E_θ in the *zy* plane. The cross-polarized waves are E_θ in the *xy* plane and *xz* plane and E_φ in the *zy* plane. Each figure is normalized by the maximum value of each characteristic. These figures confirm that the co-polarized waves in the *xy* plane and *xz* plane exhibit the well-known bidirectional characteristic and are omni-directional in the *xz* plane. Also, the cross-polarized wave has a difference of 25 dB or more from the co-polarized wave.

Figure 23 depicts the radiation patterns at the second resonant frequency. The co-polarized waves in this figure are

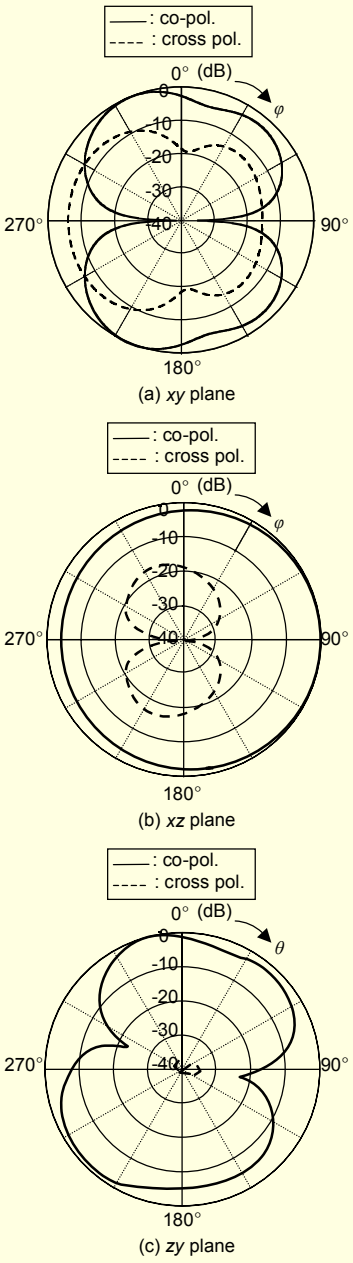

Fig. 23. Radiation patterns at the second resonant frequency.

similar to those at the first resonant frequency; however, at some angles the difference between the co-polarized wave and the cross-polarized wave becomes smaller than 25 dB. The level of the cross-polarized wave is high for one of the co-polarized waves in left side of the *xy* plane. This seems to be because the second resonant frequency is resonated by the L_{31}, L_{32}, and L_2 parts. Then, the L_{32} part is vertically located for the L_{31} and L_2 parts. Therefore, it is considered that the cross-polarized wave is caused by the current distributed on L_{32}. To suppress the cross-polarized wave level is a subject for future study.

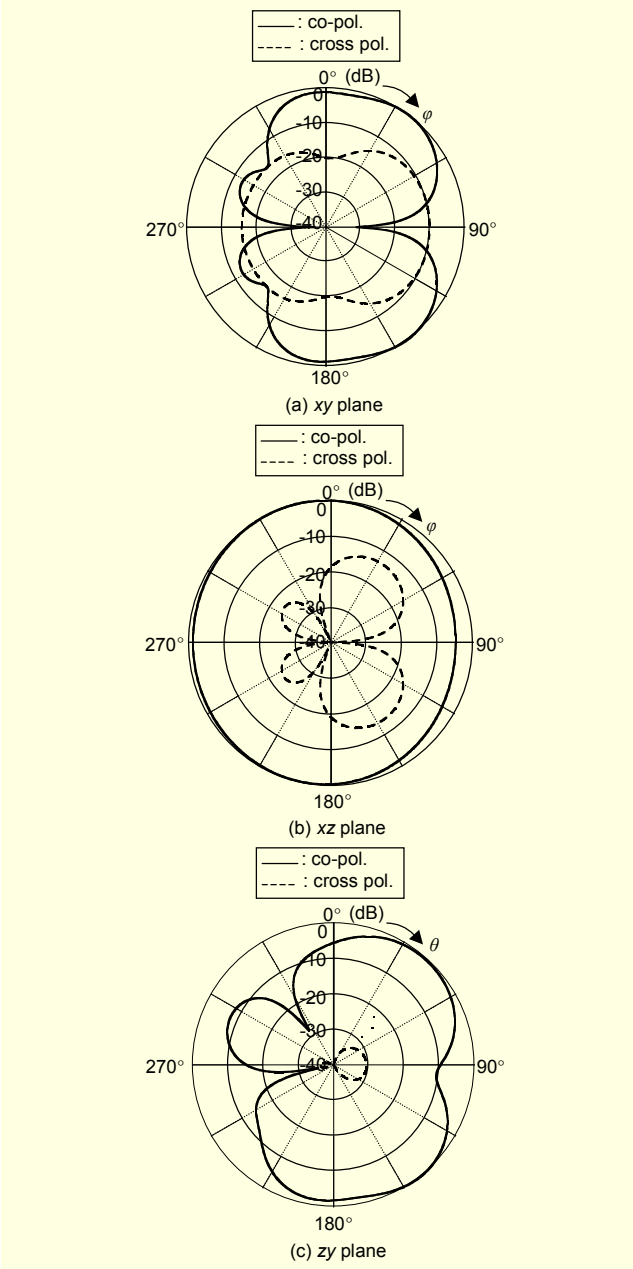

Fig. 24. Radiation patterns at the third resonant frequency.

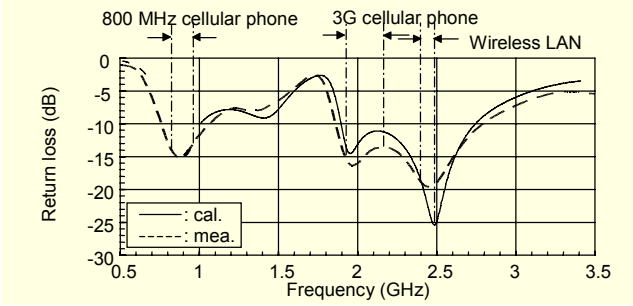

Fig. 25. Return loss of three-frequency-band antenna (L_g=85, L_d=79, W_g=60, L_1=63, L_2=45, L_{31}=12, L_{32}=13, L_c=4, c=1, h=1 mm, ε_r=4.2, e_1 = 0.953, e_2 = 0.994, e_3 = 0.866).

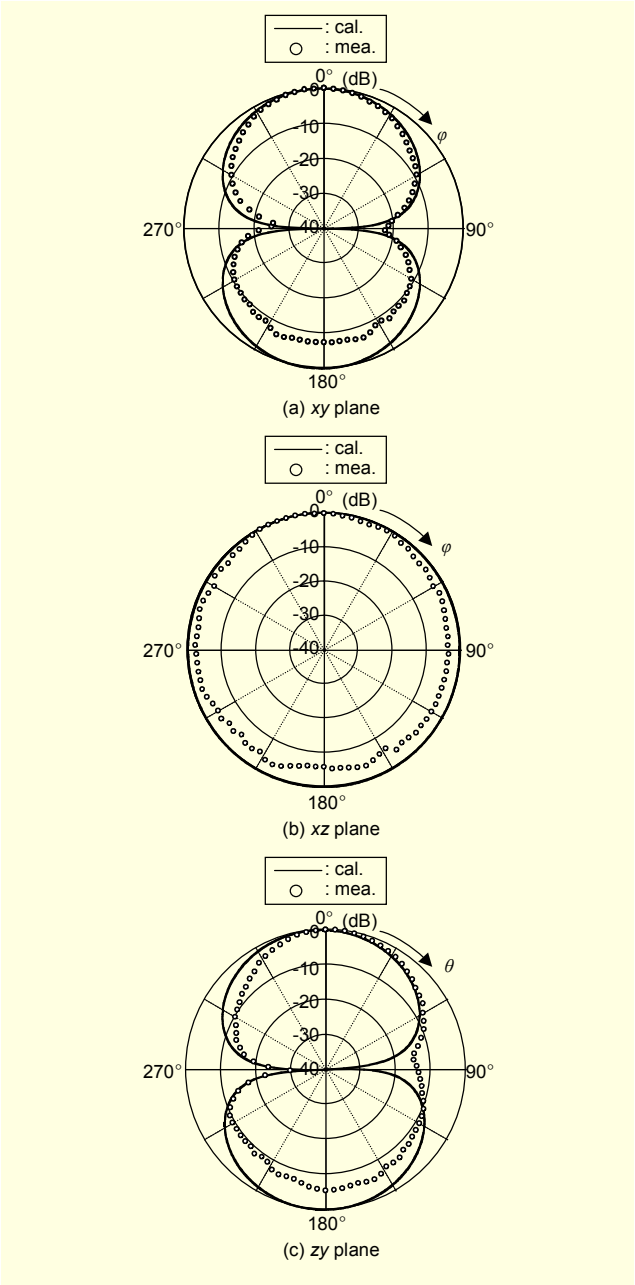

Fig. 26. Radiation patterns at the first resonant frequency.

Figure 24 illustrates the radiation patterns at the third resonant frequency. The co-polarized waves in the *xy* plane and *xz* plane become weaker around 210 degrees to 330 degrees; however, good characteristics are obtained at the other degrees. We believe the weakening of the radiation between approximately 210 degrees and 330 degrees in *xy* and *xz* planes can be explained as follows. The current of the third resonant frequency is also distributed on element 2. This is confirmed by analyzing that this current has an opposite phase for the currents distributed on L_{31} and L_{32}. The current with opposite phase is a factor which weakens the radiation around 210

degrees to 330 degrees in the *xy* and *xz* planes. In the *xz* plane, the radiation pattern is similar to that shown in Fig. 23(b). The cross-polarized wave has a pattern similar to that of the second resonant frequency. It may be that the level of the cross-polarized wave increases in the right side of the *xy* plane because the second resonant frequency is resonated by L_{31} and L_{32}. Therefore, it is likely that the cross-polarized wave is caused by current distributed on L_{32}, as in the case of the second resonant frequency. These features of the modified planar antenna with three frequency bands are similar to those of the line element planar antenna with three frequency bands.

VIII. Measured Results of Three-Frequency-Band Antenna.

Figure 25 plots the analytical and measured results of return loss of the modified planar antenna applied to three wireless communication systems. This figure indicates that the results are in agreement, and the measured results satisfy the bandwidth requirements of each communication system.

Figure 26 illustrates analytical and measured results of radiation patterns of the co-polarized wave at the first resonant frequency. The measured display the features of the pattern well and are in agreement with the analytical results. However, there are some differences at around 180 degrees in each plane. It is thought that the difference factor is due to the installation method of the cable in measuring. In the future, we will work to improve the accuracy of measurement.

Figures 27 and 28 depict the measured results of radiation patterns of the co-polarized wave at the second resonant frequency and the third resonant frequency, respectively. From these figures, it is confirmed that the measured and analytical results are in agreement.

IX. Conclusion

The basic resonant characteristics of a line element planar antenna with three frequency bands were considered in relation to changing the length of each antenna element. To improve the frequency bandwidth for broadband, a modified planar antenna with semi-elliptical elements was proposed. The effect for broadband characteristics at each resonant frequency produced by modifying the antenna element to a semi-elliptical shape was considered in relation to the eccentricity of the element.

An application of a modified planar antenna with three frequency bands, which combined an 800 MHz band cellular phone, a third-generation cellular phone, and a 2.4 GHz band wireless LAN system, was discussed as an example.

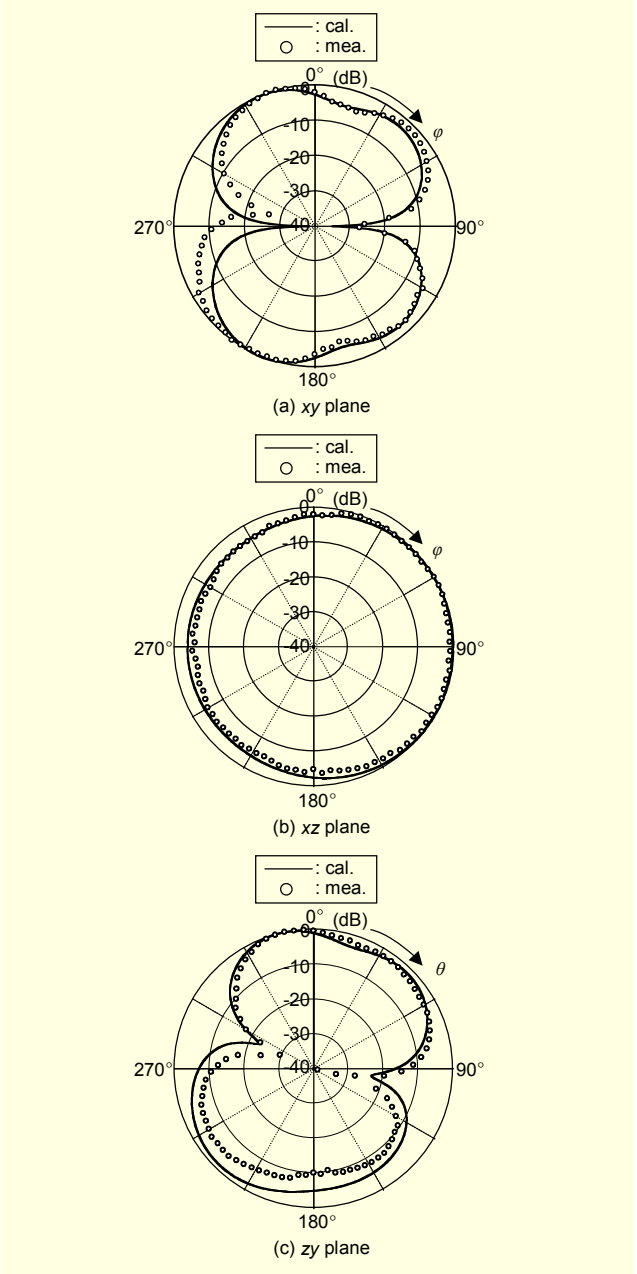

Fig. 27. Radiation patterns at the second resonant frequency.

By changing the line element in the planar antenna with three frequency bands to a semi-elliptical shape, it was possible to broaden the frequency bandwidth without deteriorating the radiation patterns. Moreover, the modified planar antenna proved to be useful as a three-frequency-band antenna.

In this study, a planar antenna with the linear polarized wave was considered. Planar antennas with both linear and circular polarized waves will be studied in the near future. Also, further miniaturization will be required when the proposed antenna is applied to many electric devices. This will also be the subject of future works.

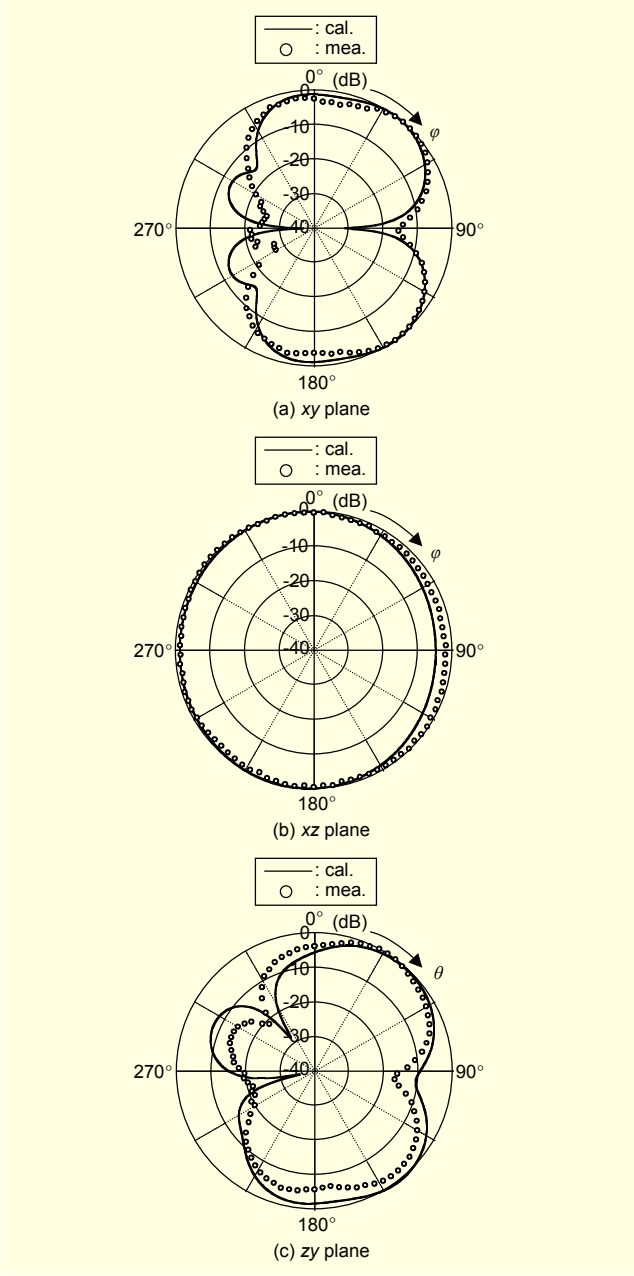

Fig. 28. Radiation patterns at the third resonant frequency.

References

[1] J. Ooe and K. Nishikawa, "Overview on Vehicle Antenna Systems," *IEICE B*, vol. J89-B, no. 9, Sept. 2006, pp. 1569-1579.

[2] T. Hori, "Broadband/Multiband Printed Antennas," *IEICE B*, vol. J87-B, no. 9, Sept. 2004, pp. 1130-1139.

[3] H. Matsui and T. Wakabayashi, "Analysis for Planar Antenna with Three-Frequency Bands Printed on Dielectric Substrate," *IEICE Technical Report*, AP2006-67, Aug. 2006.

[4] N.P. Agrawall, G. Kumar, and K.P. Ray, "Wideband Planar Monopole Antennas," *IEEE Trans. Antennas Propag.*, vol. 46, no. 2, Feb. 1998.

[5] M.C. Fabres, E.A. Daviu, A.V. Nogueira, and M.F. Bataller, "Analysis of Wideband Planar Monopole Antennas Using Characteristic Modes," *IEEE Antennas and Propagation Society International Symposium*, vol. 3, June 2003, pp.733-736.

[6] H.G. Schantz, G. Wolence, and E.M. Myszka III, "Frequency Notched UWB Antennas," *IEEE Proc. UWBST*, Nov. 2003, pp. 214-218.

[7] J.Y. Jan, L.C. Tseng, W.S. Chen, and Y.T. Cheng, "Printed Monopole Antennas Stacked with a Shorted Parasitic Wire for Bluetooth and WLAN Applications," *IEEE Antenna and Propagation Society International Symposium*, vol. 3, June 2004, pp. 2607-2610.

[8] K. Ishimiya, Z. Ying, and J. Takada, "Progress of Multi-band Antenna Technology for Mobile Phone," *IEICE Proc. Society Conference*, BS-1-2, Sept. 2006.

[9] H. Choo and H. Ling "Design of Multiband Microstrip Antennas Using a Genetic Algorithm," *IEEE Microwave and Wireless Components Letters*, vol. 12, no. 9, Sept. 2002, pp. 345-347.

[10] R. Kokubo, K. Niikura, H. Matsui, T. Wakabayashi, and K. Southisombath, "On Analysis of the Planar Antenna in FDTD Method", *IEE Technical Meeting on Electromagnetic Theory*, EMT-06-138, Oct. 2006.

[11] E. Yamashita and Y. Qian, *FDTD Analysis of Microwave Planar Circuits and Antennas*, Realize Inc., 1996.

[12] T. Uno, *Finite Difference Time Domain Method for Electromagnetic Field and Antennas*, Corona Publishing, 1998.

Hiroyasu Matsui received the BE and ME degrees in electrical engineering from Tokai University, Kanagawa, Japan, in 1988 and 1990, respectively. From 1990 to 2004, he worked for Nissan Motor Co., Ltd., as an engineer. He is currently a research student the Graduate School of Engineering at Tokai University, Japan. His research interests are various types of antennas for mobile communications. He is a member of IEICE.

Toshio Wakabayashi received the BE and ME degrees from Tokai University, in 1968 and 1970, respectively. He received the DE degree from the same university in 1985. In 1970, he joined the Faculty of Engineering, Tokai University, and since then, as a faculty member, he has engaged in research in the field of electromagnetic waves, including fields in computational electromagnetic fields, microwave circuits, and planar antenna analysis. Since 1988 he has been a professor with Tokai University. Dr. Wakabayashi is a member of the IEEE, IEICE, ITE, and the Japanese Cancer Association.